Processing and Application of Ceramics 9 [3] (2015) 139–149
DOI: 10.2298/PAC1503139S

Contribution of di- and trivalent oxides to crystal phase formations and properties of yttrium aluminosilicate glass-ceramics

Saad M. Salman, Samia N. Salama, Ebrahim A. Mahdy*

Glass Research Department, National Research Centre, Dokki, Cairo, Egypt

Received 9 June 2015; Received in revised form 8 September 2015; Accepted 25 September 2015

Abstract

The crystallization behaviour, phase composition, microhardness and chemical durability of some silicate glasses and glass-ceramics based on $LiAlSi_2O_6$-$YAlSiO_5$ system were investigated. The effects of partial replacements of $LiAlSi_2O_6$ mostly with $LiFeSi_2O_6$ and complete replacement of $YAlSiO_5$ with $CaMgSi_2O_6$ were considered. In some cases small amount of Cr_2O_3 was introduced as nucleating agent or Fe_2O_3 was partially replaced with chromium or indium oxides. The main crystalline phases formed after controlled heat-treatments of the glasses were yttrium-containing β-spodumene solid solution (ss) - $Li(Al,Y)Si_2O_6$, together with varieties of pyroxene-ss including lithium iron pyroxene-ss - $LiFeSi_2O_6$-$CaMgSi_2O_6$, augite - $Ca(Mg,Fe)Si_2O_6$, chromo-augitess, Li-aegirine - $LiFeSi_2O_6$, diopside - $CaMgSi_2O_6$ and lithium indium silicate - $LiInSi_2O_6$ phases. The Vickers' microhardness values of the studied glasses (ranged from 4610 to 6185 MPa) were greatly affected by the modifications of the glass compositions. On the other hand, the glass-ceramics' microhardness (7245–8175 MPa) was markedly improved depending on the microstructure and the nature of crystalline phases formed. The glass-ceramics have chemical stability better than those for the corresponding glasses.

Keywords: *crystallization, glass-ceramics, pyroxeness, microstructure, hardness*

I. Introduction

Glass-ceramics are forward looking materials for modern technology that has many technical applications [1]. These applications depend on the complex interrelationship of structural, compositional and processing variables [2]. It is well known that the properties of glass-ceramics are strongly dependent on the relative amounts and types of the various crystalline phases formed. The crystalline phases in the final product depend on the composition, type of nucleating agent, and the heat-treatment regime of the corresponding glass [2,3]. It is possible to obtain new glass-ceramic materials with better, and sometimes unique properties in comparison with their parent glasses, especially when the chemical composition of the basic glass and the crystallization process are properly programmed [4].

Aluminosilicate glasses containing yttria (YAS) have interesting physical properties. These glasses have high glass transition temperatures [5], interesting mechanical properties, high hardness [6] and great chemical durability [7]. The structures of yttrium aluminosilicate glasses are also of great interest in glass science to elucidate the principle of glass formation and structure [8]. Y_2O_3 was recently added to silicate and aluminosilicate glasses, allowing to improve the mechanical and thermodynamic properties [9,10] and to obtain high refractive indices, very low electrical conductivity and moderate thermal expansion coefficients. These properties make them a good alternative to borosilicate glasses currently used as sealing glass for tungsten and molybdenum [11]. Kolitsch *et al.* [12] found metastable phases for the Y_2O_3-Al_2O_3-SiO_2 system in their work for establishing the phase equilibrium of this system. Later, Lichvár *et al.* [13] also found unknown phase during their work for this system, but they did not characterize it.

An important group of glass-ceramics of high commercial value are lithium aluminium silicate (LAS) crystalline materials. They have attracted increasing attention in aviation owing to their excellent thermostability and dielectric properties [14]. The crystallization mechanism of LAS glass-ceramics was changed with more CaO and MgO additions and produced

* Corresponding author: tel: +201068704325,
fax: +20233370931, e-mail: *emahdy10@yahoo.com*

glass-ceramics with high chemical resistance and good mechanical properties [15]. As a result these glass-ceramics have found extensive application in heat exchangers; cookware or telescope mirror supports [16].

Glass-ceramics based on pyroxene group have attracted interest due to the excellent controllability of their properties. Pyroxenes are capable of a wide range of isomorphous substitution in their crystal structure and have the necessary physical and chemical characteristics, and may form the basis for production of many crystalline and glass-ceramic materials [17]. The chain silicate structure of pyroxenes enables incorporation of various cations in their structure resulting in minerals found in abundance in the nature [18].

The present work, aims to study the crystallization behaviour, and the extent of solid solution phases formed due to the heat-treatment of some glasses based on Li_2O-Al_2O_3-Y_2O_3-SiO_2 system with partial replacement of $LiAlSi_2O_6$ by $CaMgSi_2O_6$ and/or $LiFeSi_2O_6$ or $CaMgSi_2O_6$ instead of $YAlSiO_5$. The effect of introducing In_2O_3 or Cr_2O_3 at the expense of Fe_2O_3 on the phase relation and solid solution formed were also investigated. Some physico-chemical properties of the obtained materials including chemical durability and hardness were also determined.

II. Materials and methods

2.1. Preparation of glasses

The glass batches were calculated to give different proportions of stoichiometric composition $LiFeSi_2O_6$-$YAlSiO_5$ in which $LiAlSi_2O_6$ was partially replaced by $CaMgSi_2O_6$ and/or $LiFeSi_2O_6$, while $YAlSiO_5$ was completely replaced by $CaMgSi_2O_6$. In addition, in some cases small amount of Cr_2O_3 was introduced as nucleating agent (0.5 g of Cr_2O_3 was added in 100 g glass oxides) or Fe_2O_3 was partially replaced with In_2O_3 or Cr_2O_3. Details of the glass compositions are given in Table 1. The parent glasses were prepared by the conventional melt technique. Starting materials of high purity powders in the form of oxides and carbonates were taken as Li_2CO_3, $CaCO_3$, $MgCO_3$, Al_2O_3, Y_2O_3, Fe_2O_3, In_2O_3, Cr_2O_3 and SiO_2 (Fluka, ≥99.9% pure). Powders were accurately weighed and then thoroughly mixed in a ball agate mortar for about 15 minutes to ensure complete homogeneity. After mixing, batches were melted in platinum crucibles at 1350–1450 °C for 3 h with continuous stirring at intervals to achieve homogeneity. The melt batches were cast in warm stainless steel molds in the required dimensions. The prepared samples were immediately transferred to an annealing muffle furnace regulated at 500 °C, and cooled down to room temperature to minimize thermal stresses.

The progress of crystallization in the glasses was followed using double stage heat-treatment regimes. Crystallization was carried out at temperatures in the region of the main DTA exothermic peak determined for each glass. The glasses were first heated according to the DTA results at the endothermic peak temperature for 5 h, which was followed by another thermal treatment at the exothermic peak temperature for 10 h.

2.2. Sample characterization

Differential thermal analysis (DTA) was carried out using a differential thermal analyser (SETARAM Labsys™ TG-DSC16) to detect the glass transition and crystallization temperatures and determine the optimum conditions for heat treatment. The cast glass was crushed and sieved between 90 and 125 μm to produce glass powder suitable for DTA. About 20 mg of powder sample was placed in platinum crucible and subjected to a heating rate of 10 °C/min from ambient temperature to 1200 °C in a flowing high purity nitrogen environment.

Identification of the formed crystalline phases was conducted by X-ray diffraction (XRD) analysis of the powdered samples. XRD experiments were performed by X-ray diffractometer (PW1080, PANalytics, Netherlands) using Ni filtered Cu-Kα radiation with scanning speed of 2° (2θ) per minute. Diffraction pattern was recorded and the phases were identified by JCPDS numbers (ICDD-PDF2 database).

The microstructure of the heat treated samples was investigated by SEM (JEOL type JXA-840A Electron Probe Microanalyzer operated at 30 kV). The samples were fractured and the fracture positions were immersed in (1% HF + 1% HNO_3) solution for 60 s. The fracture surfaces were coated with a thin layer of gold by sputtering method. SEM was carried out to analyse the morphology of crystals in the final glass-ceramic materials.

Microhardness measurements were performed on

Table 1. Chemical composition of the glass batches

Samples	$LiAlSi_2O_6$ (LAS)	$YAlSiO_5$ (YAS)	$LiFeSi_2O_6$ (LFS)	$CaMgSi_2O_6$ (CMS)	Nucleating agent
G_1	80	20	-	-	-
G_2	50	20	30	-	-
G_3	50	-	30	20	
G_{3n}[a]	50	-	30	20	Cr_2O_3
G_{3In}	50	-	30 (In_2O_3/Fe_2O_3)	20	-
G_{3Cr}	50	-	30 (Cr_2O_3/Fe_2O_3)	20	-
G_4	40	-	30	30	-

[a] n - indicate that 0.5 g of Cr_2O_3 was added as nucleating agent in 100 g glass oxide

Table 2. Crystalline phases developed in the studied glasses

Samples	Heat-treatment [°C/h]	Crystalline phases formed
G_1	940/5–1090/10	β-spodumene-ss
G_2	885/5–1030/10	β-spodumene-ss + Li-aegirine ($LiFeSi_2O_6$)
G_3	655/5–860/10	β-spodumene + Pyroxene-ss (Li,Mg,Ca)$FeSi_2O_6$
G_{3n}	670/5–830/10	β-spodumene + Pyroxene-ss (Li,Mg,Ca)$FeSi_2O_6$
G_{3In}	675/5–880/10	β-spodumene + $LiInSi_2O_6$ + Augite
G_{3Cr}	690/5–905/10	β-spodumene + Augite-ss
G_4	640/5–850/10	β-spodumene + Diopside + Li-aegirine

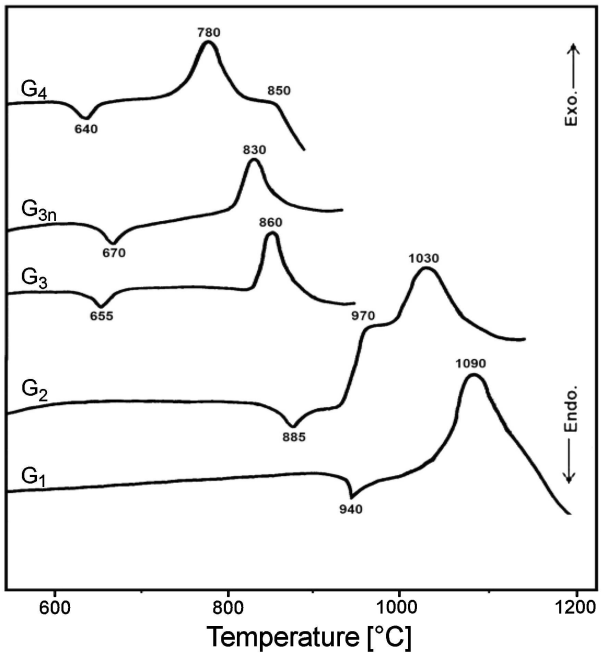

Figure 1. DTA data of the investigated glasses

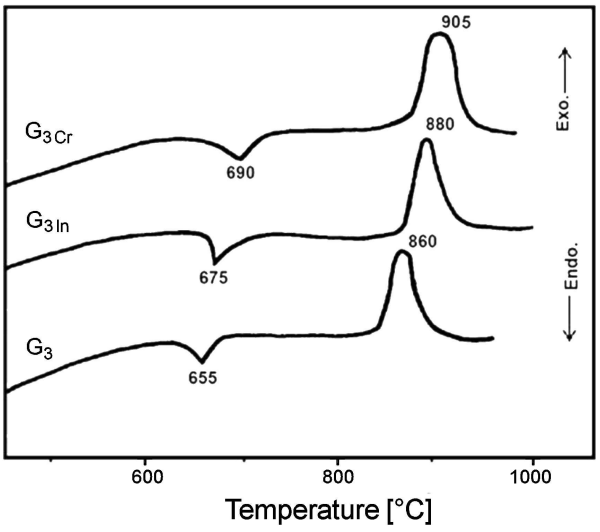

Figure 2. DTA data of the investigated glasses

mirror polished glass and glass-ceramic samples by using Vickers' microhardness tester (Shimadzu, Type-HMV, Japan). Grinding and thorough polishing were necessary to obtain polished, smooth and flat parallel surfaces of the glass and glass-ceramic samples before indentation testing. At least six indentation readings were made and measured to minimize the experimental errors and the average of values of each sample was considered. Testing was made by 100 g load and the loading time was fixed for all samples (15 s). The measurements were carried out under normal atmospheric conditions. The Vickers' microhardness value was calculated with $H_v = A(P/d^2)$ [19], where A is a constant equal to 1.8545 which takes into account the geometry of squared based diamond indenter with an angle of 136° between the opposing faces, P is the applied load and d is the average diagonal length.

The powdered method was applied to assess the chemical durability of the glass and glass-ceramic materials. The samples were crushed in an agate mortar and then sieved to obtain particles with diameter ranging between 0.63 and 0.32 mm. Then the grains were then washed by decantation in ethyl alcohol three times and dried. The dried sample was accurately weighed (1 g) in a G4-sintered glass crucible, which was then placed in a 300 ml polyethylene beaker [20]. The samples were tested for their chemical durability in 200 ml of 0.1 N HCl solution introduced into the polyethylene beaker. The polyethylene beaker with its content was covered by polyethylene cover to reduce evaporation. The experiments were carried out at 95 °C for 1 hour. The sintered glass crucible was then transferred and kept in an oven at 120 °C for 1 hour, and then transferred in a desiccator to cool down. After cooling, the total weight loss of the samples was calculated. To obtain reproducible results and minimize the experimental errors each experiment was repeated at least twice and the weight loss (in wt.%) was taken as a measure of the relative magnitude of the acid resistivity.

III. Results

3.1. Crystallization characteristics

DTA results of the investigated glass samples (Figs. 1 and 2) showed endothermic effects in the temperature range 640–940 °C, which correspond to the pre-crystallization process in the glasses. Various exothermic peaks in the temperature range 780–1090 °C, which referred to the crystallization reaction characteristic of the glasses, were also recorded. The DTA data revealed that the replacements of $LiFeSi_2O_6$/$LiAlSi_2O_6$ and/or $CaMgSi_2O_6$/$LiAlSi_2O_6$ or adding $CaMgSi_2O_6$ instead

of $YAlSiO_5$ (the samples G_1-G_4) led to the shifting of the endothermic dips and the onset of the crystallization exotherms to lower temperature values (Fig. 1). However, the addition of Cr_2O_3 as a nucleating agent (the glass sample G_{3n}) shifts the endothermic dip temperatures to higher values (Fig. 1). Also, the partial replacement of Fe_2O_3 with In_2O_3 or Cr_2O_3 in the Fe_2O_3-containing glass (i.e. the samples G_{3In} and G_{3Cr}, respectively) shifts the endothermic dip temperatures to higher values (Fig. 2).

X-ray diffraction analysis indicated that the base glass G_1 crystallized after heat treatment at 940 °C/5 h and 1090 °C/10 h, and only crystalline phase β-spodumene-ss (card no.74-1095) was formed. Moreover, the presence of yttrium phase could not be identified (Fig. 3, pattern I, Table 2). The partial replacement of $LiAlSi_2O_6$ with $LiFeSi_2O_6$ in the base glass (the sample G_2), heat-treated at 885 °C/5 h and 1030 °C/10 h led to the development of pyroxene phase of Li-aegirine - [$LiFeSi_2O_6$] type (card no.89-0225) together with β-spodumene-ss as the major phase (Fig. 3, Pattern II).

The addition of $CaMgSi_2O_6$ instead of $YAlSiO_5$ in the Fe-containing glass (the sample G_3) heated at 655 °C/5 h and 860 °C/10 h, led to the formation of pyroxene-ss of lithium iron silicate-diopside [$LiFeSi_2O_6$-$CaMgSi_2O_6$] with *d*-spacing lines close to lithium iron silicate, together with the major β-spodumene phase. However, no other phases could be detected as proved by the X-ray diffraction analysis (Fig. 3, pattern III). Figure 3 (pattern IV) indicates that for G_4 glass-ceramic sample, heat-treated at 640 °C/5 h and 850 °C/10 h, the increasing of $CaMgSi_2O_6$-content at the expense of $LiAlSi_2O_6$ led to the development of pyroxene members including diopside - $CaMgSi_2O_6$ (card no. 19-239) and Li-aegirine phases together with β-spodumene as the main crystalline phase (Table 2).

The XRD analysis of the glass-ceramic specimen G_{3In}, thermally treated at 675 °C/5 h and 880 °C/10 h revealed that the partial replacement of Fe_2O_3 with In_2O_3 led to the formation of new pyroxene-like phases as lithium indium silicate - $LiInSi_2O_6$ (card no. 33-799) and augite - $Ca(Fe,Mg)Si_2O_6$ (card no. 24-201) together with β-spodumene phase (Fig.4, pattern II). However, the partial exchange of Fe_2O_3 with Cr_2O_3 led to the crystallization of pyroxene solid solution of augite - $Ca(Mg,Fe)Si_2O_6$ type (card no.76-544) together with the major β-spodumene phase as indicated by the X-ray diffraction analysis of the glass G_{3Cr}, heat-treated at 690 °C/5 h and 905 °C/10 h (Fig. 4, pattern III, Table 2).

The addition of small amount of Cr_2O_3 (0.5 wt.%), as nucleating agents, greatly improved the crystallization of the glass. Thus, the X-ray diffraction analysis showed that amount of iron-containing pyroxene phase was significantly increased by introducing small amount of Cr_2O_3 to the glass (the sample G_{3n}) heat-treated at 670 °C/5 h and 830 °C/10 h (Fig. 5, Table 2).

SEM micrographs of the fractured surfaces of the crystallized glasses are presented in Figs. 6 and 7. They

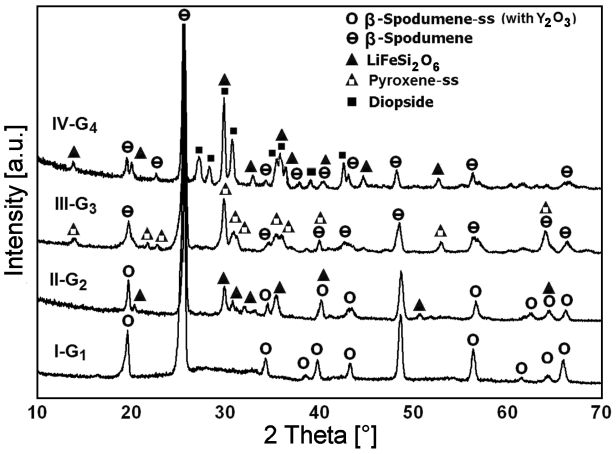

Figure 3. X-ray diffraction analysis of the crystallized glasses G_1-G_4

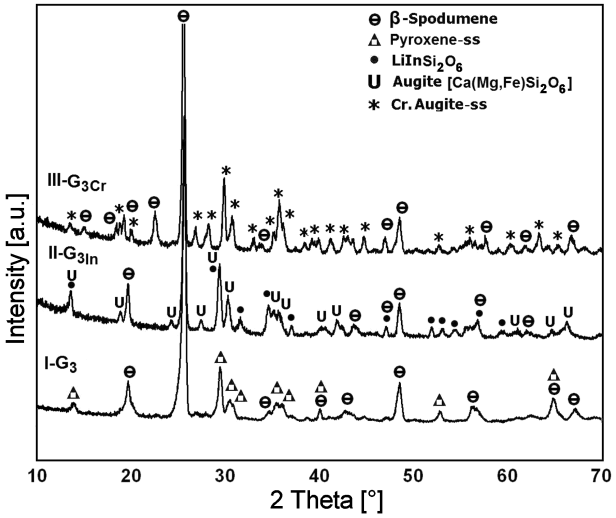

Figure 4. X-ray diffraction analysis of the crystallized glasses G_3, G_{3In} and G_{3Cr}

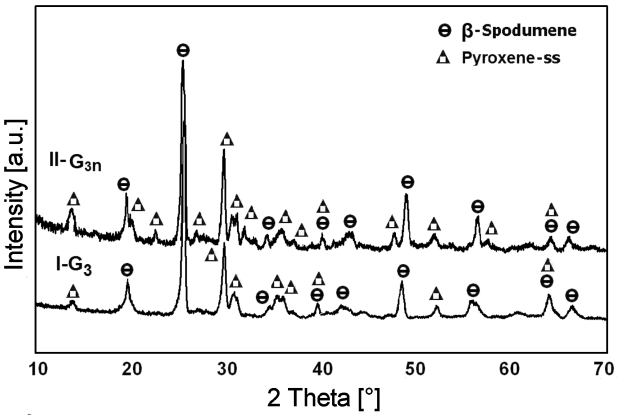

Figure 5. X-ray diffraction analysis of the crystallized glasses G_3 and G_{3n}

clearly show that volume crystallization of fine fibrous with needle-like crystals was developed for the crystalline base glass (the sample G_1) (Fig. 6a). The replacement of $LiAlSi_2O_6$ with $LiFeSi_2O_6$ in the base glass (the

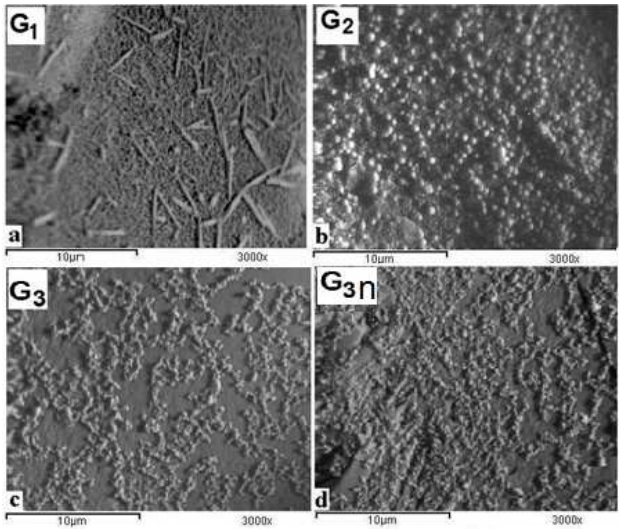

Figure 6. SEM micrograph of fracture surface of heat treated glass-ceramics: a) G_1, b) G_2, c) G_3 and d) G_{3n}

sample G_2) led to volume crystallization and formation of very small spherulite-like units (Fig. 6b). However, the complete substitution of $YAlSiO_5$ with $CaMgSi_2O_6$ in the Fe-containing glass (the sample G_3) led to the formation of numerous tiny aggregates-like units (Fig. 6c). The addition of minor amount of Cr_2O_3, as nucleating agent (the sample G_{3n}), led to bulky crystallization and formation of very tiny aggregates (Fig. 6d). The partial replacement of Fe_2O_3 with In_2O_3 (the sample G_{3In}) enable development of fine fibrous crystals with tiny aggregates (Fig. 7a). However, the involvement of Cr_2O_3 at the expense of Fe_2O_3 (the sample G_{3Cr}) led to volume crystallization and formation of dense fine microstructure (Fig. 7b).

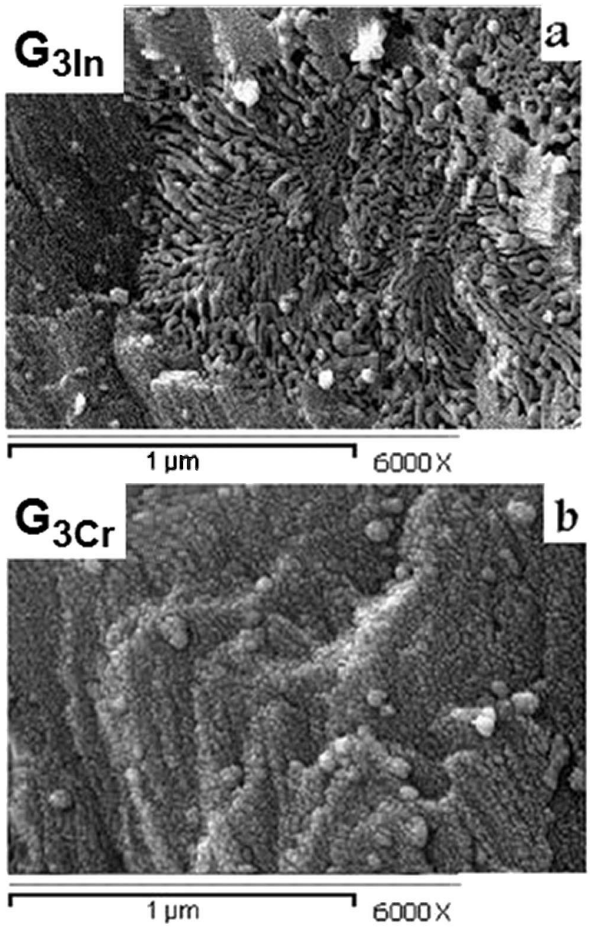

Figure 7. SEM micrograph of fracture surface of heat treated glass-ceramics: a) G_{3In} and b) G_{3Cr}

3.2. Microhardness

The microhardness properties of the resulting glass and glass-ceramics were determined by Vickers' microhardness. The obtained data for the microhardness of the investigated glass and glass-ceramic materials are graphically represented in Fig. 8. The Vickers' microhardness values of the investigated glass samples are ranging from 4610 to 6185 MPa. The data revealed that the partial replacements of $LiFeSi_2O_6/LiAlSi_2O_6$ and/or $CaMgSi_2O_6/LiAlSi_2O_6$ or adding $CaMgSi_2O_6$ instead of $YAlSiO_5$ led to the decrease in the microhardness values, while the partial replacements of Fe_2O_3 with In_2O_3 or Cr_2O_3 caused the increase in the microhardness values of the investigated glasses (Fig. 8). However, in crystalline state the microhardness values for the glass-ceramics were found to be in the ranged from 7245 to 8175 MPa. From the obtained data, it was noticed that all modification processes in the glass-ceramic compositions led to the increase in the microhardness values of the resultant crystalline materials (Fig. 8).

Entering of small amount of the Cr^{3+} ions, as nucleating agent, in the glass sample G_{3n} also gave rise to the increasing of microhardness values for the investigated glass and its glass-ceramic sample (Fig. 8).

3.3. Chemical durability

The chemical durability characterization of the glasses and corresponding glass-ceramics was conducted in order to evaluate the chemical resistance in hot acidic media. Figure 9 shows the chemical stability of the examined samples tested in 0.1 N HCl solution at 95 °C. The results of weight loss of glass samples showed that the base glass sample (G_1) was more durable than all other glass samples. Therefore, the replacements of $LiFeSi_2O_6/LiAlSi_2O_6$ and/or $CaMgSi_2O_6/LiAlSi_2O_6$ or the addition of $CaMgSi_2O_6$ instead of $YAlSiO_5$ led to the decrease in the chemical resistance of the resultant glasses. While the partial replacements of In_2O_3/Fe_2O_3 or Cr_2O_3/Fe_2O_3 led to the increase in the durability of the obtained glasses by acid solution (Fig. 9).

For the crystalline samples, the obtained data revealed that the chemical durability of the examined crystalline samples was improved by the replacement of $LiFeSi_2O_6/LiAlSi_2O_6$ and/or $CaMgSi_2O_6/LiAlSi_2O_6$ or $CaMgSi_2O_6/YAlSiO_5$ (Fig. 9). Also, introducing of In_2O_3 or Cr_2O_3 at the expense of Fe_2O_3 led to the increase in the chemical resistance of the crystalline materials against the acid attack.

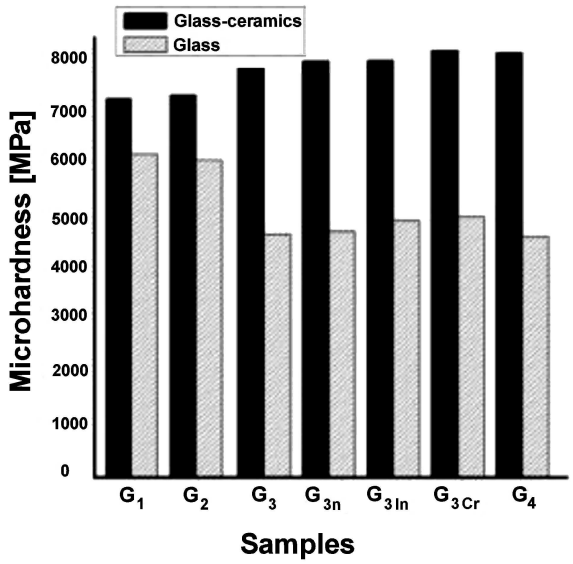

Figure 8. Microhardness of the investigated glasses and their glass-ceramics

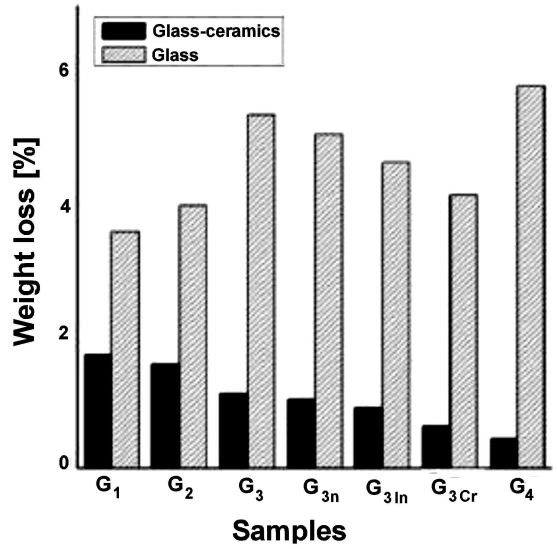

Figure 9. The chemical durability of the investigated glasses and their glass-ceramics

The addition of minor amount of Cr_2O_3 (0.5 wt.%), as nucleating agent, in the examined sample G_{3n} led to the decrease in the weight loss by the acidic solution for the studied glass and its corresponding glass-ceramic sample (Fig. 9).

IV. Discussion

4.1. DTA Study

The structure of multicomponent silicate glasses is based on a polymeric network with coexisting cations, which may act as modifier or as charge compensating cations needed for balancing the charge deficit of oxygen neighbours. This situation occurs when trivalent cations are substituted to silicon in the polymeric network. Glass properties may be strongly affected depending whether cations are network modifiers or charge compensators [21].

The results of DTA curves show well-defined glass transition ranges and exothermic peaks corresponding to the crystallization of possible crystalline phases. The locations of the main endothermic and exothermic peaks of the base glass, G_1, were detected at higher temperatures than in other glasses (Figs. 1 and 2).

The replacement of $LiFeSi_2O_6$ with $LiAlSi_2O_6$ in the base glass, G_1, clearly indicates that the endothermic and the onset of crystallization exothermic peaks are shifted toward the lower temperature values with increasing of Fe_2O_3 contents (present in $LiFeSi_2O_6$ molecule) instead of Al_2O_3 (present in $LiAlSi_2O_6$ molecule). This drop of temperature could be attributed to the fact that the addition of Fe_2O_3 in the glasses greatly favours the formation of non-bridging oxygen atoms [22]. Therefore, the increase of Fe_2O_3 content led to the decrease in the coherency of the glass network compared to that arising by the presence of Al_2O_3. The decreasing of SiO_2 content and increasing of Li_2O also may contribute to this drop. Agarwal *et al.* [23] stated that the decreasing of SiO_2 content led to the decrease in density of cross-linking of the silicate units in the glass structure which decreases the cohesiveness of the network and hence the glass transition temperature. On the other hand, Li_2O can contribute to form non-bridging oxygen atoms, therefore, a drop of temperature could be expected.

The addition of $CaMgSi_2O_6$ at the expense of $YAlSiO_5$ or $LiAlSi_2O_6$ in the iron-containing glasses led to the shift of the endothermic peak temperatures toward lower values. This can be explained on the basis that the glass transition temperature decreased with divalent modifier cations (CaO and MgO) present in the glasses instead of trivalent former cations Al_2O_3 and Y_2O_3. In other words, the presence of trivalent oxides Al_2O_3 and Y_2O_3 in the glasses led to the obtaining of a stronger structure, therefore, a higher transition temperature could be expected [24].

The addition of trivalent In_2O_3 or Cr_2O_3 at the expense of Fe_2O_3 in the glasses remarkably changed the glass transition temperatures as well as crystallization temperatures. This may be attributed to the ionic field strength of the two trivalent element added which possess a higher field strength than that of iron. This may account for the increase of the coherency of glass structure [25]. Therefore, the endothermic peak temperatures of the investigated glasses were shifted towards higher temperatures by the addition of different trivalent ions instead of Fe_2O_3.

The addition of small amount of Cr_2O_3, as nucleating agent, in glass sample G_{3n} increase the coherency of the network in the glass structure, raise the temperature at which the crystallization starts, increasing the crystallization tendency of the glasses and leading to the increase of the number of crystallization centres, thus forming fine grained microstructure [1].

4.2. X-ray diffraction for the crystallization study

The X-ray diffraction analysis (Fig. 3, pattern I) revealed that the base glass, G_1, crystallized to β-spodumene-ss phase. The presence of Y_2O_3 in the glass enhanced the development of β-spodumene, as the main crystalline phase, which was formed directly without the transformation from β-quartz into β-spodumene [26]. The present data is in agreement with the previous studies by Zheng *et al.* [27]. They found that β-spodumene ($Li_2O \cdot Al_2O_3 \cdot 4\,SiO_2$) was observed directly without transformation from β-quartz to β-spodumene. As the temperature increases from 820 to 970 °C, the content of β-spodumene increases gradually.

The present result revealed that there is a great affinity of β-spodumene-$LiAlSi_2O_6$ to accommodate Y_2O_3 in its structure and to form solid solution. The displacement of the major characteristic *d*-spacing lines may support the suggestion that Y^{3+} was incorporated in the β-spodumene structure giving rise to the probable formula; $Li(Al_{0.79}Y_{0.21})Si_2O_6$. However, no other phases containing yttrium could be detected (Fig. 3, pattern I). Ahmad *et al.* [28] suggested that yttrium ion is substituted with an aluminium ion and oxygen content remains constant. But the main contradiction to this suggestion is that the ionic radii of Y^{3+} (0.1 nm) differ greatly from the ionic radii of Al^{3+} (0.06 nm). Furthermore, despite the difference in radius, the substitution is permitted by the crystal chemistry. Singh *et al.* [29] reported that the addition of Y_2O_3 in any glass composition increase the stability of the glasses without forming any detrimental phase during the heat treatment.

The obtained results indicated also that the partial replacement of $LiAlSi_2O_6$ with $LiFeSi_2O_6$ in the base glass (the sample G_2) led to the development of pyroxene phase of Li-aegirine - $LiFeSi_2O_6$ type together with β-spodumene-ss as the major phase (Fig. 3, pattern II). Lithium iron pyroxene was described by Salman [30] who showed that iron oxide tends to be accommodated in the lithium silicate structure rather than lithium borate to form a Li-aegirine phase $LiFeSi_2O_6$. Lithium iron pyroxene has great theoretical and technological importance in glass-ceramic technology.

The addition of $CaMgSi_2O_6$ instead of $YAlSiO_5$ in the iron-containing glasses (the sample G_3) does not lead to the formation of different phases than those obtained from the crystallized glass G_2 ($CaMgSi_2O_6$-free sample). However, the amount of Li-aegirine phase was increased as indicated from the increase of the intensities of their *d*-spacing lines of the XRD analysis together with β-spodumeness phase (Fig. 3, pattern III). The displacement of the major characteristic *d*-spacing lines of the pyroxene variety towards higher 2θ values (Fig. 3, pattern III) may support the suggestion that diopside molecules ($CaMgSi_2O_6$) were accommodated in the lithium iron pyroxene (Li-aegirine) host structure giving rise to the formation of the probable pyroxene solid solution formula $(Li_{0.52}Ca_{0.24}Mg_{0.24})FeSi_2O_6$.

Salman and Salama [31] confirmed that a great extent of solid solution phase could be formed between two pyroxenes - diopside and $LiFeSi_2O_6$. Simultaneously, at higher $CaMgSi_2O_6$ content at the expense of $LiAlSi_2O_6$ (the sample G_4) no complete solid solution between diopside and Li-aegirine could be formed and the diopside-$CaMgSi_2O_6$ phase is exsolved, i.e. the two phases diopside - $CaMgSi_2O_6$ and Li-aegirine - $LiFeSi_2O_6$ are detected together with the major β-spodumene phase as confirmed by the X-ray diffraction analysis of the glass G_4 (Fig. 3, Pattern IV).

The state of iron, its coordination and concentration in the glasses mainly determined the nature of the phases formed especially at high Li_2O + Fe_2O_3 content. Iron oxide can be present in the glass as ferrous (Fe^{2+}) and ferric (Fe^{3+}) ions, and their ratio depends on the glass composition and melting conditions [31]. In silicate glasses, the ferric cations may occupy octahedral FeO_6 and tetrahedral FeO_4 sites [32], while the ferrous cations occupy only octahedral sites which decrease by increasing the iron content [33]. The presence of appreciable amounts of Li_2O together with Fe_2O_3 in the present glasses, greatly favour the formation of non-bridging oxygen atoms. The high concentrations of non-bridging oxygen atoms in silicate glass will favours Fe^{2+} in the network-forming position as $Fe^{2+}O_4$.

The partial replacements of Fe_2O_3 with In_2O_3 in glass composition (the sample G_{3In}) led to crystallization of the lithium indium silicate - $LiInSi_2O_6$ phase together with β-spodumene (major) phase and iron-containing pyroxene phase of augite type (Fig. 4, pattern II). The structure of augite is similar to that of diopside. In this case a limited partial replacement of silica by Fe^{3+} ions seemed to be taking place in the tetrahedral position, which was accompanied by introducing Li^+ ions to preserve electrical neutrality, leading to the pyroxene formation of augite phase having the probable formula $Ca(Mg_{0.49}Li_{0.51})(Fe_{0.34}Si_{0.66})_2O_6$.

The partial swap of Fe_2O_3 by Cr_2O_3 (the sample G_{3Cr}) led to the formation of β-spodumene as the major phase together with pyroxene solid solution phase of chromo-augite type having the following probable formula $Ca(Mg_{0.33}Li_{0.67})(Fe_{0.17}Cr_{0.17}Si_{0.66})_2O_6$. A wide variety of ionic substitutions occur in the members of the pyroxene group. The complexity of this group is exhibited by the wide isomorphism of the various elements in the expandable pyroxene formula [18] resulting in minerals found in abundance in the nature, such as diopside ($CaMgSi_2O_6$), aegirine ($NaFeSi_2O_6$), and augite $(Ca,Na)(Mg,Fe,Al,Ti)(Si,Al)_2O_6$.

From the XRD patterns (Fig. 4, pattern III), it has to be noted that participation of Cr^{3+} ions in Fe_2O_3-containing glass (the sample G_{3Cr}) did not affect type of the phases but it induced change of the relative intensities of the pyroxene phase. This may indicate that the crystallization rate of the iron-containing pyroxene-ss was increased by the involvement of Cr_2O_3. Rezvani *et al.* [34] summarized the role of chromium oxide as follows: Cr_2O_3 can induce a glass-in-glass phase sepa-

ration or directly precipitate from molten glass during cooling stage as some form of chromium spinel crystallites; it greatly assisted the formation of final pyroxene or diopside-like phases. Chromium oxide is characterized by a low solubility in silicate glass melts, resulting in the direct formation of Cr-based spinels, which then appear as nuclei for pyroxene glass-ceramics formation [35].

The results showed also that the introduction of minor amount of Cr_2O_3, as nucleating agent, into the glass sample G_{3n} favours pyroxene crystallization of the glass as indicated by the development of the intensities of their d-spacing lines in the XRD (Fig. 5). Karamanov *et al.* [36] stated that Cr_2O_3 is very effective nucleating agent in high iron content glasses. They proved that a small percentage of Cr_2O_3 strongly affects the spinel formation and enhances the degree of crystallization of iron containing silicate glasses.

SEM micrographs (Figs. 6 and 7) showed that the replacement processes led to the volume crystallization and formation of fine grained microstructures. Salman *et al.* [37] observed that the presence of iron oxide increases the number of crystallization centres and stimulates the crystallization of the glass during the reheating process giving rise to the volume crystallization of fine grained microstructures. Karamanov *et al.* [36] claimed also that addition of 0.7% Cr_2O_3 enhances the spinel formation and consequently nucleation rate causing a higher degree of crystallization and finer structures in these glass-ceramics with the major crystalline phase of pyroxene.

4.3. Microhardness

The hardness value is usually defined as the ratio of the indentation load and either the surface or projected area of residual indents. The standard hardness tests are vital in nearly all areas of materials science and engineering. On the other hand, a good understanding of the relationship between the hardness and tensile properties of materials is very important [38].

From the Vickers' microhardness values of the glass samples, the obtained data shows that the base glass sample (G_1) has the highest value among all glass samples (Fig. 8). The microhardness values, on the other hand, were decreased with low Y_2O_3 and Al_2O_3-contents in the glass batches. However, the introduction of trivalent oxides In_2O_3 or Cr_2O_3 at the expense of Fe_2O_3 in the glass sample led to the increase of the microhardness values. The microhardness, therefore, is a bond sensitive property [39], which provides an insight on the nature of the chemical bonding in a material. So the strong network forming role of Al_2O_3 in aluminosilicate glasses increases with the Al_2O_3-content in the glasses. Therefore, high Al_2O_3 containing glasses display high hardness values [40]. Varshneya [41] revealed that the addition of alkalis to the silicate glasses decreased their hardness [42] presumably because the connectivity of the glass structure decreased.

Sohn *et al.* [43] revealed that the hardness of silicate glass-ceramics increased due to the formation of fine grained microstructure by which the crystal size plays an important role in preventing the propagation of the cracks in the whole structure. The microhardness of crystallized glasses depends not only on the type of precipitating phases but also on their size, shape, and natural wetting as well on the emergence or absence of internal cracks. However, the degree of crystallinity should be also taken into consideration [44].

Dependence of microhardness on the replacement processing for different glass samples is shown in Fig. 8. The microhardness value for the base crystalline sample G_1 is 7245 MPa, which increases slowly after replacement with $LiFeSi_2O_6$ and/or $CaMgSi_2O_6$ molecules (the samples G_2-G_4). This may be due to that, the presence of iron oxide led to more nucleation sites [37] during the first stage of heat treatment, and thus achieving a very fine microstructure as compared with that of Fe_2O_3-free crystalline sample, G_1 (Fig. 6a). The development of high mechanical strength pyroxene-like crystals as Li-aegirine, diopside, iron-containing pyroxenes and their solid solutions are also considered. The microhardness of glass-ceramics generally increased with the increase of crystallinity, smaller crystalline aggregates as well as formation of fine microstructure [45]. The microstructure mostly represents the major influence on the mechanical properties of the glass ceramic materials [46].

The data also indicate that the glass-ceramic samples containing In_2O_3 or Cr_2O_3 instead of iron oxide (the samples G_{3In} and G_{3Cr}, respectively) had higher microhardness values than that for the sample G_3 - free of In_2O_3 or Cr_2O_3 (Fig. 8). This may be due to the formation of high mechanical pyroxene member phases together with β-spodumene phase. Glass-ceramics based on pyroxenes have attracted interest due to the excellent controllability of their properties. Pyroxenes are capable of a wide range of isomorphous substitutions in their crystal structure and having a distinct physical and chemical characteristic [47].

The results also showed that, the introduction of minor amount of Cr_2O_3, as nucleating agent, in the sample G_{3n} led to the increase of the crystallization tendency of the glasses, and strongly enhanced volume crystallization with the formation of very fine grained microstructure (Fig. 6d), this was followed by an increase in the microhardness values of the glass and its crystalline sample as compared with that of the Cr_2O_3-free sample, i.e. G_3, (Fig. 8). Enrique *et al.* [48] stated that the presence of Cr_2O_3 supported earlier crystallization of pyroxene-like crystals and the formation of a more homogeneous glass-ceramic material characterized with relatively high mechanical strength.

4.4. Chemical durability

The chemical stability of the examined glasses was decreased by the additions of $LiFeSi_2O_6$ or $CaMgSi_2O_6$ instead of $LiAlSi_2O_6$ or $CaMgSi_2O_6$/$YAlSiO_5$ replace-

ment (the samples G_2-G_4). While, the partial replacements of In_2O_3/Fe_2O_3 or Cr_2O_3/Fe_2O_3 (the samples G_{3In} and G_{3Cr}, respectively) led to the increase of the chemical durability of the obtained glasses (Fig. 9). In yttrium aluminosilicate glasses, the rare earth ions in these glasses had similar structural function as that of the aluminium ions [23]. While, conventional ternary yttrium aluminosilicate glasses that incorporate of divalent cation modifiers (e.g. Ca and Mg), is usually attributed to stronger bonding of the Y^{3+} cations, and to the lower contrast in bond strengths between bridging and non-bridging oxygen [24]. Bunker *et al.* [49] stated that, in the glass dissolution, the divalent cations are leached from the glass surface by exchange with protons in the solution in the early stage of the reaction.

The chemical durability of glass-ceramics is quite different from that of glasses. It must be viewed as a multiphase system with each phase having individual corrosion characteristic and possible unique reactions at the phase boundary [50]. The greater mobility of alkali metal ions in the glass phase as compared with that of similar ions incorporated in crystal phases will lead to greater reactivity of the glass phase and hence to inferior resistance to chemical attack. The achievement of high chemical durability in glass-ceramics indicates that, the chemical composition of the crystalline phases obtained favour good stability. McMillan [1] had indicated that, the glass ceramic, in general, possess good chemical stability and that they compare favourably in this respect with other ceramic type materials.

All modifications in the glass compositions by replacement processes led to great improvements in the chemical durability of the resultant glass-ceramics (Fig. 9). This may be attributed to that the replacement processes led to support the development of the highly durable low reactive pyroxene member [18] with formation of fine microstructure e.g., Li-aegirine, diopside, lithium indium silicate, iron-containing pyroxenes and their solid solutions, together with the presence of low reactive lithium aluminosilicate crystals [51], e.g. β-spodumene, which had been formed as dominant crystalline phase. MacMillan [1] pointed out that lithium aluminosilicate glass-ceramics of medium thermal expansion are quietly unaffected by exposure of chlorine or hydrogen chloride gases for a period of 6 h at 800 °C. Varieties of pyroxene phases and their solid solution containing Fe^{3+}, Mg^{2+} and/or Ca^{2+} show variable resistance towards the acid attack. The solubility of both the formed crystals and the residual glass phase in leaching solution has almost an equally important influence on the chemical stability of glass ceramics [1]. Varieties of pyroxene phases and their solid solution containing Fe^{3+}, Mg^{2+} and/or Ca^{2+} show variable resistance towards the acid attack. The solubility of both the formed crystals and the residual glass phase in leaching solution has almost an equally important influence on the chemical stability of glass ceramics [1].

The presence of Cr_2O_3, as nucleating agent, in the Fe_2O_3-containing sample (G_{3n}) improved also the chemical stability of the both glass and crystalline sample (Fig. 9). This may be attributed to the formation of a coherent glass structure. This led to the decrease of the leachability of the nucleant glasses. Other explanation was also due to the crystallization of better chemical stability materials with dense nonporous very fine microstructure [1] of the pyroxene-like phase.

V. Conclusions

Glass-ceramic materials of high chemical resistance and good mechanical properties were successfully prepared by introducing $LiFeSi_2O_6$ and/or $CaMgSi_2O_6$ molecules at the expense of $LiAlSi_2O_6$ or $CaMgSi_2O_6$ instead of $YAlSiO_5$ in the glasses based on Li_2O-Al_2O_3-Y_2O_3-SiO_2 system. The same trends of the properties were also obtained in the presence of In_2O_3 or Cr_2O_3. The main crystalline phases, formed after controlling heat-treatment are yttria-containing β-spodumene-ss - $[Li(Al,Y)Si_2O_6]$ together with varieties of pyroxene phases including Li-aegirine, diopside, lithium indium silicate and iron-containing pyroxene solid solution including lithium iron silicate-ss - $LiFeSi_2O_6$-$CaMgSi_2O_6$, augite - $Ca(Mg,Fe)Si_2O_6$ and chromo-augite-ss. The replacement processes greatly change the microhardness values and chemical durability data of the glasses. However, in the case of crystalline state the microhardness and chemical durability of the glass-ceramics were greatly improved due to the development of varieties of pyroxene phases and their solid solutions with the formation of fine grained microstructure. The addition of Cr_2O_3, as nucleating agent in the selected glass, was also improved the properties of the glass and its corresponding glass-ceramic. The present results provided valuable information about the role of glass oxide constituents and heat treatment applied in determining the crystalline phase formations, the nature of the solid solution formed as well the chemical and mechanical properties of the resultant materials.

Acknowledgements: The authors are grateful to SAIF, Kochi for providing the instrumental data, UGC and to the Principal, CMS College, Kottayam, Kerala for providing the necessary facilities.

References

1. P.W. McMillan, *Glass-ceramics*, Academic Press, New York, 1979.
2. W. Holand, G.H. Beall, *Glass-Ceramic Technology*, The American Ceramics Society, Westerville, OH, USA, 2002.
3. P. James, "Glass-ceramic: New compositions and uses", *J. Non-Cryst. Solids*, **181** (1995) 1–15.
4. L. Karolina, C.K. Katarzyna, B.L. Maria, "Thermal and spectroscopic characterization of glasses and glass-ceramics of Li_2O-Al_2O_3-SiO_2 (LAS) system", *J. Mol. Struct.*, **1068** (2014) 275–282.

5. I.H. Arita, DS. Wilkinson, GR. Purdy, "Crystallization of yttria-alumina-silica glasses", *J. Am. Ceram. Soc.*, **75** (1992) 3315–3320.
6. I. Pozdnyakova, N. Sadiki, L. Hennet, V. Cristiglio, A. Bytchkov, G.J. Cuello, J.P. Coutures, D.L. Price, "Structures of lanthanum and yttrium aluminosilicate glasses determined by X-ray and neutron diffraction", *J. Non-Cryst. Solids*, **354** (2008) 2038–2044.
7. N. Sadiki, J.P. Coutures, C. Fillet, J.L. Dussossoy, "Crystallization of lanthanum and yttrium aluminosilicate glasses", *J. Nucl. Mater.*, **348** (2006) 70–78.
8. D. Jincheng, "Molecular dynamics simulations of the structure and properties of low silica yttrium aluminosilicate glasses", *J. Am. Ceram. Soc.*, **92** (2009) 87–95.
9. Y. Zhang, A. Navrotsky, "Thermochemistry of glasses in the Y_2O_3-Al_2O_3-SiO_2 system", *J. Am. Ceram. Soc.*, **86** (2003) 1727–1732.
10. A. Makimishima, T. Shimoira, "Alkaline durability of high elastic modulus alumino-silicate glasses containing Y_2O_3, La_2O_3 and TiO_2", *J. Non-Cryst. Solids*, **38-39** (1980) 661.
11. J.E. Shelby, S.M. Minton, C.E. Lord, M.R. Tuzzolo, "Formation and properties of yttrium aluminosilicate glasses", *Phys. Chem. Glasses*, **33** (1992) 93.
12. U. Kolitsch, H.J. Seifert, T. Ludwig, F. Aldinger, "Phase equilibria and crystal chemistry in the Y_2O_3-Al_2O_3-SiO_2 system", *J. Mater. Res.*, **14** (1999) 447–555.
13. P. Lichvár, P. Sajgalík, M. Liska, D. Galusek, "CaO-SiO_2-Al_2O_3-Y_2O_3 glasses as model grain boundary phases for Si_3N_4 ceramics", *J. Eur. Ceram. Soc.*, **27** (2007) 429–436.
14. F. Luo, D.M. Zhu, W.C. Zhou, "A two-layer dielectric absorber covering a wide frequency range", *Ceram. Int.*, **33** (2007) 197–200.
15. A.M. Hu, M. Li, D.L. Mao, "Growth behavior, morphology and properties of lithium aluminum silicateglass-ceramic with different amounts of CaO, MgO and TiO_2 additives", *Ceram. Int.*, **34** (2008) 1393–1397.
16. Y.M. Sung, S.A. Dunn, J.A. Koutsky, "The effect of boria and titania addition on the crystallization and sintering behavior of Li_2O-Al_2O_3-4 SiO_2 glass", *J. Eur. Ceram. Soc.*, **14** (1994) 455–462.
17. R.M. Thompson, R.T. Downs, "Model pyroxenes II: Structural variation as a function of tetrahedral rotation", *Am. Mineral.*, **89** (2004) 614–628.
18. W.A. Deer, R.A. Howie, J. Zussman, "An introduction to the rock-forming minerals", *Third ELBS impression*, Hong Kong, Common Wealth, Printing Press Ltd., 1992.
19. R.L. Smith, G.E. Sandland, "An accurate method of determining the hardness of metals, with Particular reference to those of a high degree of hardness", *Proceedings of the Institution of Mechanical Engineers*, **1** (1922) 623–641.
20. L. Wu, Y. Li, Y. Teng, G. Meng, "Preparation and characterization of borosilicate glass-ceramics containing zirconolite and titanite crystalline phases", *J. Non-Cryst. Solids*, **380** (2013) 123–127.
21. G. Calas, L. Cormier, L. Galoisy, P. Jollivet, "Structure-property relationships in multicomponent oxide glasses", *Comptes Rendus Chim.*, **5** (2002) 831–843.
22. T.J. Kiczenski, C. Ma, E. Hammarsten, D. Wilkerson, M. Affatigato, S. Feller, "A study of selected physical properties of alkali germinate glasses over wide ranges of composition", *J. Non-Cryst. Solids*, **272** (2000) 57–66.
23. A. Agarwal, S. Sanghi, R. Bala, S. Khasa, "Influence of SiO_2 on the structural and dielectric properties of $ZnO \cdot Bi_2O_3 \cdot SiO_2$ glasses", *J. Integr. Sci. Technol.*, **3** (2015) 6–13.
24. T. Schaller, J.F. Stebbins, "The structural role of lanthanum and yttrium in aluminosilicate glasses: Al^{27} and O^{17} MAS NMR study", *J. Phys. Chem. B*, **102** (1998) 10690–10697.
25. R.H. Doremus, *Glass Science*, 2nd ed., John Wiley and Sons Inc., New York, 1994.
26. M. Guedes, A.C. Ferro, J.M.F. Ferreira, "Nucleation and crystal growth in commercial LAS compositions", *J. Eur. Ceram. Soc.*, **21** (2001) 1187–1194.
27. W. Zheng, J. Cheng, L. Tang, J. Quan, X. Cao, "Effect of Y_2O_3 addition on viscosity and crystallization of the lithium aluminosilicate glasses", *Thermochim. Acta*, **456** (2007) 69–74.
28. S. Ahmad, T. Ludwig, M. Herrmann, M.M. Mahmoud, W. Lippmann, H.J. Seifert, "Phase evaluation during high temperature long heat-treatments in the Y_2O_3-Al_2O_3-SiO_2 system", *J. Eur. Ceram. Soc.*, **34** (2014) 3835–3840.
29. K. Singh, N. Gupta, O.P. Pandey, "Effect of Y_2O_3 on the crystallization of SiO_2-MgO-B_2O_3-Al_2O_3 glasses", *J. Mater. Sci.*, **42** (2007) 6426–6432.
30. S.M. Salman, "Crystallization of alkali iron pyroxene $LiFeSi_2O_6$ in Li_2O-SiO_2 glasses containing iron oxide", *Interceram.*, **30** (1981) 48–51.
31. S.M. Salman, S.N. Salama, "Pyroxene solid solutions crystallized from CaO-MgO(Li_2O, Fe_2O_3)-SiO_2 glasses", *Ceram. Int.*, **12** (1986) 221–228.
32. C.R. Kurkjian, E.A. Sigety, "Coordination of Fe^{3+} in glass", *Phys. Chem. Glasses*, **9** (1968) 73–83.
33. S.M. Salman, "Thermal expansion characteristics of some iron containing glasses and their corresponding crystalline materials", *Thermochim. Acta*, **81** (1984) 125–137.
34. M. Rezvani, B. Eftekhari-Yekta, M. Solati-Hashjin, V.K. Marghussian, "Effect of Cr_2O_3, Fe_2O_3 and TiO_2 nucleants on the crystallization behaviour of SiO_2-Al_2O_3-CaO-MgO (R_2O) glass-ceramics", *Ceram. Int.*, **31** (2005) 75–80.
35. G. Müller, *Low Thermal Expansion Glass Ceramics*, Springer-Verlag, Ed. H. Bach, Berlin, 1995.
36. A. Karamanov, P. Pisciella, M. Pelino, "The effect

of Cr_2O_3 as a nucleating agent in iron-rich glass-ceramics", *J. Eur. Ceram. Soc.*, **19** (1999) 2641–2645.
37. S.M. Salman, F. Mostafa, "Crystallization of alkali-iron-borosilicate glasses", *Sprechsaal*, **118** (1985) 622–676.
38. I. Brooks, P. Lin, G. Palumbo, G.D. Hibbard, U. Erb, "Analysis of hardness-tensile strength relationships for electroformed nanocrystalline materials", *Mater. Sci. Eng. A*, **491** (2008) 412–419.
39. J. Zarzycki, *Glass and Vitreous State*, Cambridge Univ. Press, New York, Port Chester, USA, 1991.
40. J.F. MacDowell, *Alumina in Glasses and Glass-ceramics, Reprinted from Alumina Chemicals Science and Technology Handbook*, Am. Ceram. Soc. Inc., USA, 1990.
41. A.K. Varshneya, *Fundamentals of Inorganic Glasses*, Academic Press, London, UK, 1994.
42. H. Scholze, *Glass-nature Structure, and Properties*, Springer-Verlag, New York, 1990.
43. S.B Sohn, S.Y. Choi, Y.K. Lee, "Controlled crystallization and characterization of cordierite glass-ceramics for magnetic memory disk substrate", *J. Mater. Sci.*, **35** (2000) 4815–4821.
44. H.A. Miska, *Ceramics and Glasses*, Engineered Materials Handbook, 4ASM Int. 4, 1991.
45. F.J. Torres, J. Alarcon, "Effect of additives on the crystallization of cordierite-based glass-ceramics as glazes for floortiles", *J. Eur. Ceram. Soc.*, **23** (2003) 817–826.
46. J. Henry, R.G. Hill, "The influence of lithia content on the properties of fluorphlogopite glass-ceramics, II-Microstructure hardness and machineability", *J. Non-Cryst. Solids*, **319** (2003) 13–30.
47. R.M. Thompson, R.T. Downs, G.J. Redhammer, "Model pyroxenes III: Volume of C2/c pyroxenes at mantle P, T, and X", *Am. Mineral.*, **90** (2005) 1840–1851.
48. M. Enrique, G. Alexander, I. Jose, "Crystallization behavior of glasses in the system of Na_2O-CaO-MgO-Fe_2O_3-Al_2O_3-SiO_2 with high contents of nickel oxide", *J. Non-Cryst. Solids*, **353** (2007) 366–373.
49. B.C. Bunker, "Molecular mechanism for corrosion of silica and silicate glasses", *J. Non-Cryst.Solids*, **179** (1994) 300–308.
50. W.J. McCracken, "Corrosion of glass-ceramics", in *Corrosion of Glass, Ceramics and Ceramic Super Conductors*, Ed. by D.E. Clark & B. Zoitos, Noyes Publications, Park Ridge, New Jersey, USA, 1992.
51. D.C. Boyd, P.S. Danielson, D.A. Thompson, *Glass Kirk-Othmer Encyclopedia of Chemical Technology*, 4th Ed., John Wiley, and Sons Inc, New York, USA, 1994.